XI International Conference on Textile Composites and Inflatable Structures
STRUCTURAL MEMBRANES 2023
C. Lázaro, R. Rossi and R. Wüchner (Eds)

SHAPE-ADAPTIVE CLIMATE LOADING OF TENSILE SURFACE STRUCTURES

ZBYNĚK ZAJAC[*], ROSTISLAV LANG[†] AND IVAN NĚMEC[†]

[*,†] Institute of Structural Mechanics, Faculty of Civil Engineering
Brno University of Technology
Veveří 331/95, 602 00 Brno, Czech Republic
e-mail: zajac.z@fce.vutbr.cz, web page: https://www.fce.vutbr.cz/en

[*,†] FEM consulting, s.r.o.
Veveří 331/95, 602 00 Brno, Czech Republic
e-mail: fem@fem.cz, web page: https://www.fem.cz/?lang=en

Key words: Algorithm, Snow Load, Tensile Surface Structures

Summary. This paper deals with climate loading of tensile surface structures. The approaches for the snow load calculation were summarized and a new usage for tensile surface structures based on established procedures has been proposed. The snow load distribution and accumulation was presented in the form of an algorithm implemented in a finite element software. The results of the algorithm for snow load accumulation were verified on simple examples with vertical, inclined and curved surfaces.

1 INTRODUCTION

To design the proper shape of a membrane structure may be a demanding task even for a highly experienced professionals. There is a tremendous amount of available shapes, membrane materials and ways of construction and there are also a large number of factors that must be taken into consideration and evaluated during the design process. A truly important and probably decisive factor is climate loading. In the case of conventional structures, the climate load also constitutes a substantial part of the loading, however the inclination and deformability of the surfaces in such structures is low. On the other hand, the highly inclined surfaces of the tensile surface structure combined with their great deformability makes the task of load effect evaluation rather difficult.

Great deformability is probably the biggest disadvantage of membrane materials. In the case of insufficient design, despite the surface prestress, an unfavorable phenomenon called ponding effect may occur. This phenomenon is potentially dangerous, because the snow is accumulating on the membrane. If the amount of concentrated load exceeds the tensile strength of the material a tear may appear in the fabric. [1]

There are many software tools that facilitate the design process of membrane structures therefore the final shape is found faster and the structure is safer. This research

contributes to the general knowledge by providing a tool to assess the shape of the tensile surface structure for the snow load accumulation occurrence. Load volume distribution is equally important due to uneven loading of the structure. Moreover, the effect of load in the areas filled with accumulated snow is complex. The lateral pressure of the accumulated snow is induced and should be considered. In the case of tensile surface structures, highly variable inclination makes this evaluation a very challenging task.

1.1 Snow load standards

Generally, standards for snow load are still under development compared to the standards for loading of conventional structures. European standards, valid in the Czech Republic, do not mention tensile surface structures at all. Fortunately, there are excellent guides for experts, such as [2], that summarize recommendations and provide solutions for complex structures.

Usually, snow load is considered as a uniform load on a projected area. This approach is sufficient for conventional buildings without considering snow accumulation. Although, the snow load shape coefficient μ is established by the standards, it is a difficult task to determine a proper value in the case of tensile surface structures due to the changing inclination. The amount of snow load is usually reduced by μ, because snow slips from the steep surfaces. There are some recommendations on how to consider accumulated snow, but a more exact way is to calculate the amount of snow that has slipped.

The behavior of accumulated snow is similar to the behavior of soils, thus the snow mechanics is analogous. Its action is spatial so there are not only vertical actions σ_z of the load, but also lateral actions σ_x and σ_y. The vertical action σ_z is dependent on height h:

$$\sigma_z = h \cdot \rho \cdot g \tag{1}$$

where ρ is fluid density and g is the standard gravitational acceleration for the surface of the Earth.

The lateral pressure may be calculated from the material properties, specifically from the angle of internal friction ϕ that represents the shearing resistance of the material. Another mechanical property is angle of repose α, that means the inclination angle of a stable slope. The internal friction angle is strongly dependent on the initial density and is approximately equal to α in the loosest state of the material [3]. The lateral pressures σ_x and σ_y could be calculated as:

$$\sigma_x = \sigma_y = K_a \cdot \sigma_z \tag{2}$$

So, if snow is considered as cohesionless and the surface as frictionless, it is possible to calculate the active earth pressure coefficient K_a according to Rankine's theory:

$$K_a = \frac{1-sin\phi}{1+sin\phi} \tag{3}$$

A study of the angle of repose [4] shows that this material property is strongly dependent on fall height, snow temperature, volume-weighted mean projected area diameter

and circularity. Moreover, this dependency is nonlinear. The research [4] shows that ϕ of snow collected outdoors varies from 20° to 40° for sufficiently low temperature. This range is in accordance with values presented in [5] where the authors proved that the angle of internal friction is higher as the temperature increases. A similar conclusion [6] stated that a higher water content lowers the internal friction angle of snow. This implies that more densely accumulated snow induces higher lateral pressure.

Publication [7] conservatively recommends to consider a value of ϕ equal to 15° for a lateral pressure exerted by snowdrift on a vertical wall.

1.2 Principle of the virtual work

According to the general principle, the variation of the overall virtual work must be equal to zero which implies:

$$\begin{aligned} \delta W^{int} &= \delta W^{ext} \\ {}^{t+\Delta t}\boldsymbol{\sigma}\ \delta {}^{t+\Delta t}\boldsymbol{\epsilon}\, {}^{t+\Delta t}\mathrm{dV} &= {}^{t+\Delta t}\mathbf{R} \end{aligned} \tag{4}$$

where δW^{int} and δW^{ext} are the variations of the internal and external virtual work, $\boldsymbol{\sigma}$ is the Cauchy stress tensor, $\delta\boldsymbol{\epsilon}$ is the variation of the infinitesimal strain tensor over the unknown volume and $\mathbf{R}$ is virtual work of the external forces in the new configuration at time $\mathrm{t} + \Delta\mathrm{t}$.

Because of the unknown configurations, the equation is rewritten to the actual configuration with known strain and stress, using Updated Lagrangian formulation. In the next step, the linearization is performed by neglecting high-order terms due to a complicated nonlinear function of the unknown displacement increment. The final linearized equilibrium equations in matrix notation are as follows:

$$\int_{{}^{t}\mathrm{V}} {}^{t}\mathbf{C}_{t}\boldsymbol{\epsilon}\delta_{t}\boldsymbol{\epsilon}^{t}\mathrm{dV} + \int_{{}^{t}\mathrm{V}} {}^{t}\boldsymbol{\sigma}\delta_{t}\boldsymbol{\eta}^{t}\mathrm{dV} = {}^{t+\Delta t}\mathbf{R} - \int_{{}^{t}\mathrm{V}} {}^{t}\boldsymbol{\sigma}\delta_{t}\boldsymbol{\epsilon}^{t}\mathrm{dV} \tag{5}$$

where $\mathbf{C}$ denotes the constitutive material law, $\boldsymbol{\epsilon}$ and $\boldsymbol{\eta}$ are the linear and nonlinear part of the Green-Lagrange strain tensor, respectively.

If the load is assumed as dependent on deformation:

$${}^{t+\Delta t}\mathbf{R} = \int_{{}^{t}\mathrm{V}} {}^{t+\Delta t}\mathbf{f}^{\mathrm{V}}\ \delta\mathbf{u}^{\mathrm{V}}\ {}^{t}\mathrm{dV} + \int_{{}^{t}\mathrm{S}} {}^{t+\Delta t}\mathbf{f}^{\mathrm{S}}\ \delta\mathbf{u}^{\mathrm{S}}\ {}^{t}\mathrm{dS} + \sum {}^{t+\Delta t}\mathbf{F}\delta\mathrm{u} \tag{6}$$

where ${}^{t}\mathrm{V}$ and ${}^{t}\mathrm{S}$ are the volume and the surface area respectively, ${}^{t+\Delta t}\mathbf{f}^{\mathrm{V}}$, ${}^{t+\Delta t}\mathbf{f}^{\mathrm{S}}$, ${}^{t+\Delta t}\mathbf{F}$ are volume, surface and nodal forces dependent on the nodal displacement variation $\delta\mathbf{u}$.

The middle part of Equation 6, specifically the integral $\int_{{}^{t}\mathrm{S}} {}^{t+\Delta t}\mathbf{f}^{\mathrm{S}}\ \delta\mathbf{u}^{\mathrm{S}}\ {}^{t}\mathrm{dS}$, represents the external nonlinear surface forces that change during the calculation.[8]

2 METHODOLOGY

In order to facilitate the snow load calculation a whole process was developed, automated and implemented in cooperation with FEM Consulting, s.r.o. and Dlubal Software GmbH. A previous research that focused on ponding effect detection on deformed surfaces was previously developed. As was discussed in section 1.1, the consequences of water accumulation may cause vast and expensive damages. Hence, an algorithm for ponding effect detection was developed and implemented in finite element analysis software RFEM.

Generally, the lowest local points on a deformed surface are found. If such a point exists, the algorithm scans for a catchment area of the local minimum. As soon as the catchment area is found, the pond is defined as well as its drainage point. This particular point determines the surface level of the pond. The information about the deformed mesh combined with the water level enables the calculation of a sufficiently accurate volume of the pond. This research was summarized and presented in the 20^{th} International conference of numerical analysis and applied mathematics ICNAAM 2022, Heraklion.

Algorithm 1: Surface level of redistributed snow

Data: p, γ, $A_{p,i}$, μ, z_D, z_B
$h_i = \frac{p}{\gamma} \cdot \mu_i$;
$h_{s,i} = \frac{p}{\gamma} \cdot (\mu_{max} - \mu_i)$;
$V_{max} = \sum_{i=1}^{n} (h \cdot \mu_{max} \cdot A_{p,i})$;
$V_{acc} = \sum_{i=1}^{n} (h_{s,i} \cdot A_{p,i})$;
if $V_{acc} > 0$ **then**
  $a \leftarrow z_B - h_D$; $b \leftarrow z_D$;
  $Err = \mathbf{abs}(a - b)$;
  while $Err > 0.001$ **do**
    $c = \frac{(a+b)}{2}$; /* Surface level of accumulated snow */
    $V_c = 0$;
    forall n **do**
      if $z_i > c$ **then**
        $h_i = h_i + (z_i - c)$; /* Column of snow on element */
        $V_c = V_c + h_i \cdot A_{p,i}$; /* Volume of redistributed snow */
      end
    end
    $V = V_{acc} - V_c$;
    if $V < 0$ **then** $b = c$ **else** $a = c$;
    $Err = \mathbf{abs}(a - b)$;
  end
  $z_N = \frac{(a+b)}{2}$
end

The algorithm was modified in order to facilitate snow load distribution calculation. An important input for Algorithm 1 is a graph of the dependence of shape coefficient μ on inclination of the roof, load intensity p and specific weight γ. Firstly, the inclination of each element is calculated and the corresponding μ determined. The snow was assumed to be liquid for the redistribution in order to verify the volume.

Algorithm 1 describes the procedure where n is the number of the catchment area elements, h_i is the height of snow on the i^{th} element, $A_{p,i}$ is the projected area in the global Z, V_{acc} is the volume of accumulated snow, V_{max} is the maximum volume of snow, z_D is the drainage surface level (for liquids), z_B the coordinate Z of the lowest point, z_i the coordinate Z of the gravity center of the i^{th} element and z_N is the new surface level. Basically, the inner cycle is based on the bisection method whose advantages are the convergence certainty and error control.

2.1 Snow load effect

As described in Section 1.1, the action of accumulated snow is not only in the direction of gravity. In order to simplify the solution, the snow in the accumulated area is assumed to be liquid. The action of isotropic hydrostatic pressure has equal magnitude in every direction and is represented by tensor $\boldsymbol{\sigma}_\mathbf{h}$ in Equation 7. However, this would represent only a melted snow as a liquid.

In order to include the material characteristics of fresh or heavy snow, the active pressure coefficient K_a was implemented in Equation 2, so the tensor $\boldsymbol{\sigma}$ in Equation 7 includes lateral pressures where $\sigma_x = \sigma_y$. This tensor is transformed to a local coordinate system of an element in Equation 7 where $\mathbf{T}$ and $\mathbf{T}^\mathbf{T}$ is the transformation matrix and its transposition, respectively.

$$\boldsymbol{\sigma}_\mathbf{h} = \begin{bmatrix} \sigma & 0 & 0 \\ 0 & \sigma & 0 \\ 0 & 0 & \sigma \end{bmatrix} \Rightarrow \boldsymbol{\sigma} = \begin{bmatrix} \sigma_x & 0 & 0 \\ 0 & \sigma_y & 0 \\ 0 & 0 & \sigma_z \end{bmatrix} \rightarrow \boldsymbol{\sigma}^* = \mathbf{T}\ \boldsymbol{\sigma}\ \mathbf{T}^\mathbf{T} = \begin{bmatrix} \sigma_{xx} & \tau_{xy} & \tau_{xz} \\ \tau_{yx} & \sigma_{yy} & \tau_{yz} \\ \tau_{zx} & \tau_{zy} & \underbrace{\sigma_{zz}}_{\vec{f}_z} \end{bmatrix} \tag{7}$$

Finally, the element is loaded in a local coordinate system by the vector $\vec{f}_z$ obtained from the stress tensor $\boldsymbol{\sigma}^*$ and other components are neglected.

3 RESULTS AND DISCUSSION

3.1 Verification example 1 - cylinder

In order to verify the algorithm a simple example was calculated. A cylinder 1.5 m high with a 0.25 m radius was subjected to load calculated by the algorithm. The surfaces of the cylinder were 0.01 m thick and supported in the local direction z so the contact stresses corresponds directly to the load. The dimensions and results are summarized in Figure 1.

The input value of shape coefficient μ is 0.8, the specific weight γ is $4.0\,\mathrm{kNm}^{-3}$ and the load intensity p was $5.0\,\mathrm{kNm}^{-2}$. According to the equation in Algorithm 1 the height of snow h_s on a flat surface is 1.0 m. The active pressure coefficient K_a was conservatively set to 0.5 in order to analytically verify the results.

Therefore, the local load acting on the base $p_z = h_s \cdot p \cdot \mu = 4.0\,\mathrm{kNm}^{-2}$ and the local lateral load $p_z = h_s \cdot p \cdot \mu \cdot K_a = 2.0\,\mathrm{kNm}^{-2}$. The final sum of loads in global direction Z is 0.786 kN which corresponds to the analytical solution $\sum F_z = \pi \cdot r^2 \cdot p_z = 0.785\,\mathrm{kN}$.

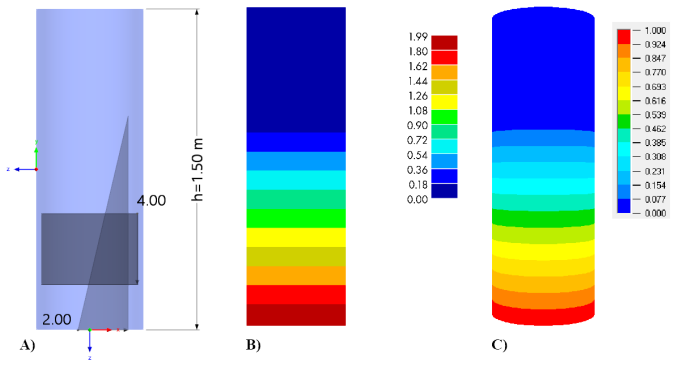

Figure 1: Cylinder loaded with snow. A) Corresponding load for verification (kNm^{-2}), B) Load (kNm^{-2}) calculated and applied by Algorithm 1, C) Height of snow (m).

3.2 Verification example 2 - truncated cone

Secondly, a similar analysis was performed using a truncated cone 5.0 m high with the lower base radius $r_l = 0.25$ m and the upper base radius $r_u = 0.75$ m hence the angle $\theta = 84.29°$. The thickness and support remained the same as in Section 3.1. The dimensions and results are summarized in Figure 2.

The values for the input were $\mu = 0.8$, $\gamma = 4.0\,\mathrm{kNm}^{-3}$ and $p = 2.0\,\mathrm{kNm}^{-2}$, hence the height of snow h_s before redistribution is 0.4 m. It follows that the maximum volume of snow $V_{max} = \pi \cdot r^2 \cdot h_s = 0.707\,\mathrm{m}^3$ and the sum of loads $\sum F_z = V_{max} \cdot \gamma = 2.827\,\mathrm{kN}$. The analytical solution corresponds to the value 2.825 kN obtained from finite element solution.

The accumulated snow height h_w in the truncated cone obtained from the analysis is 1.864 m and the corresponding radius r_w is 0.436 m. The volume was confirmed analytically:

$$V = \frac{\pi \cdot h_w}{3} \cdot (r_l^2 + r_l \cdot r_w + r_w^2) = 0.707\,\mathrm{m}^3 \tag{8}$$

The components of stress in the case of $K_a = 0.5$ are $\sigma_z = 7.456\,\mathrm{kNm}^{-2}$ and $\sigma_x = \sigma_y = 3.728\,\mathrm{kNm}^{-2}$. In order to verify the inner calculation from the finite element software, the stress components were transformed to the local coordinate system of the inclined elements:

$$\sigma_z^{'} = \frac{\sigma_y + \sigma_z}{2} + \frac{\sigma_y - \sigma_z}{2} \cdot \cos 2\theta = 3.764\,\mathrm{kNm}^{-2} \tag{9}$$

$$\tau_{yz}^{'} = \frac{\sigma_y - \sigma_z}{2} \cdot \sin 2\theta = 0.369\,\mathrm{kNm}^{-2} \tag{10}$$

The finite element analysis with corresponding load from Figure 2A calculated by Equations 9 and 10 confirmed the results printed in Figure 2B obtained from the static analysis with the load given by the algorithm.

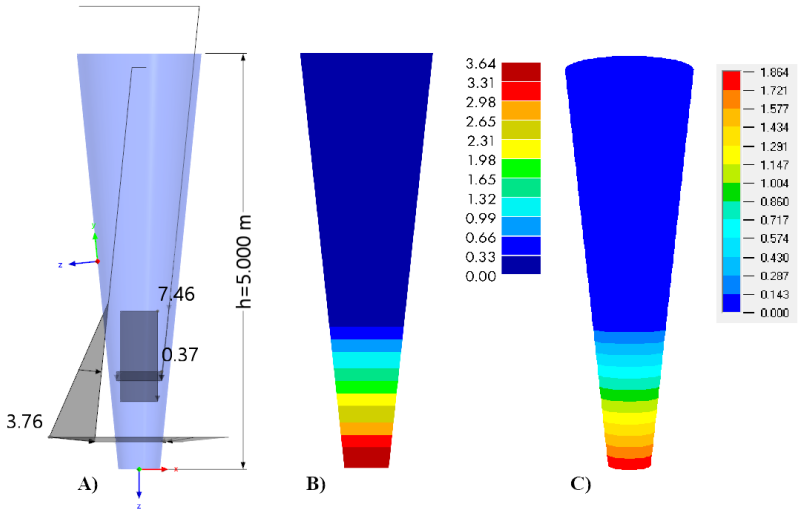

Figure 2: Truncated cone loaded with snow. A) Corresponding load for verification (kNm^{-2}), B) Load (kNm^{-2}) calculated and applied by Algorithm 1, C) Height of snow (m).

3.3 Verification example 3 - funnel

The previous Sections 3.1 and 3.2 dealt with the verification of the algorithm. The final part demonstrates its usage in order to prevent design flaws of tensile surface structures.

As a demonstrative example the Dresden main railway station roof was chosen. The failure of the membrane material of the funnel, damage extent and repair possibilities were described in [1] or [9].

The paper focuses on a critical part of the structure. Only the funnel with blocked drain in Figure 3 was modeled and loaded in order to clarify the action of the snow load. The height of the funnel was 3.00 m, the radii of the lower r_l and upper r_u base were 0.25 m and 1.00 m respectively, hence the inclination before form-finding calculation was 75.96°.

PVC type I was the chosen material of the funnel and the local coordinate system is shown in Figure 3. In order to compare only the internal forces n_x induced by the applied load, there was an effort to exclude the pre-stressing forces. However, in order to perform the form-finding process the small amount of pre-stress 0.1 kNm^{-1} had to be prescribed. So the final results presented in Figure 3 and 4 are almost unaffected by the pre-stress.

The projected surface area A_z in global Z is equal to $\pi\,\mathrm{m}^2$. The load intensity $2.0\mathrm{kNm}^{-2}$ combined with shape coefficient 0.8 equals to load $1.6\,\mathrm{kNm}^{-2}$. The analytically calculated sum of forces $\sum F_Z = 5.03$ kN corresponds to the finite element solution 5.01 kN. This implies that the total amount of snow is not affected during the run of Algorithm 1.

In Figure 3, there are internal axial forces n_x of the funnel loaded by projected load in global Z on the left side. The distribution of internal forces compared to the funnel loaded by Algorithm 1 in the middle, indicates the importance of the load accumulation effect inclusion. The axial forces are not only higher in the case of solution B), but also the percentage of maximum values distribution. The right side of Figure 3 shows the surface level of the accumulated snow in the funnel.

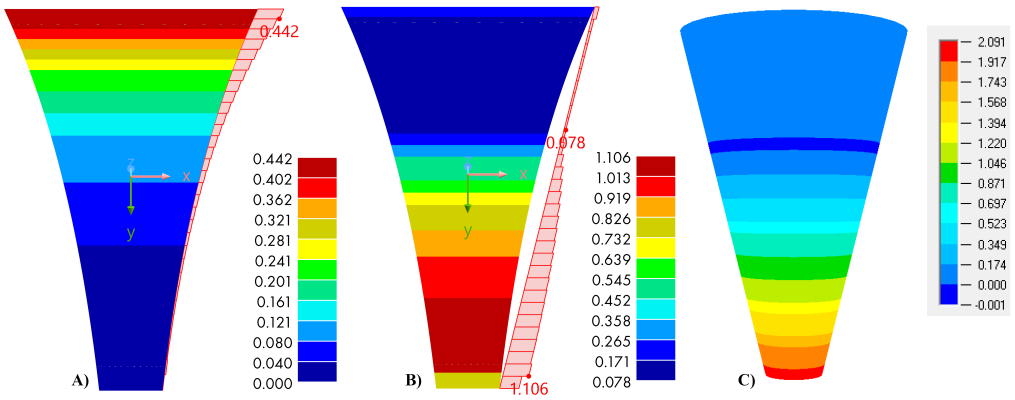

Figure 3: Internal axial forces $n_x(\mathrm{kNm}^{-1})$ of loaded funnel A) by projected load in global Z, B) by Algorithm 1, C) Height of accumulated snow (m).

The most important outcome is apparent in Figure 4. There are forces direction orientation of the principal internal forces n_1 and n_2 in the membrane surface. On the left

side, the vertical direction in the local direction y prevails. This orientation does not corresponds to reality. On the other hand, the results B) provide a quite precise internal action. As was hypothesized, the direction of horizontal forces in local direction x prevails and stretch out the funnel in width. This results in higher stress on the seams in the perpendicular direction.

It is important to mention that this state may occur only as a consequence of an inappropriate design when the drain is blocked. So until this failure occurs, some of the defects in a membrane material may remain hidden. If the accumulated snow melts and then freezes, the already disturbed material is ripped in order to release the internal tension.

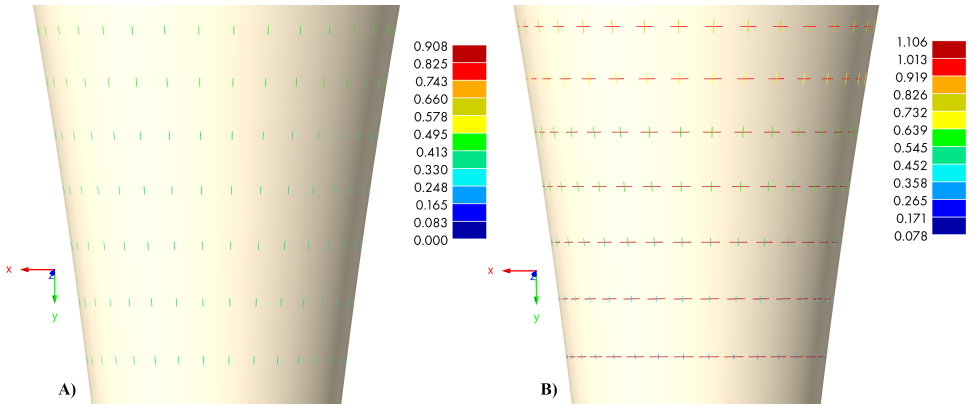

Figure 4: Forces direction orientation of loaded funnel A) by projected load in global Z, B) by Algorithm 1.

4 CONCLUSION

This paper focuses on climate shape-adaptive loading of tensile surface structures that are characterized by strong geometric nonlinearity. A consistent load prescribed before calculation does not reflect the variability during the iterations. The shape changes during the calculation and so should the load distribution.

In order to facilitate the snow load evaluation, Algorithm 1 was developed and implemented. The automation of the task is necessary due to the high curvature of membrane surfaces and the variability of shapes. Even though the snow slips from highly inclined surfaces, part of the amount may stay in place. Hence, the complex analysis including a catchment area determination and amount of snow calculation should be performed. Specifically the action of the accumulated snow was examined. An approach similar to the soil analysis was evaluated and implemented. The algorithm was verified in three separate examples with similar shape in order to compare the results with analytical solutions.

The most important outcome is the confirmation that the forces direction orientation in the blocked funnel may be the cause of the damage. It is a financially and time demanding task to repair such a structure. The algorithm could facilitate the design process and help to prevent this unfortunate incident.

REFERENCES

[1] Weller, F., Common problems in the design and construction of membrane structures. *8th International Conference on Textile Composites and Inflatable Structures - STRUCTURAL MEMBRANES 2017*, 147—177 (2018).

[2] Forster, B. and Mollaert, M. European design guide for tensile surface structures, Brussels, ISBN 90–8086–871–X, (2004).

[3] Terzaghi, K. *Theoretical Soil Mechanics*. John Wiley and Sons, Inc., New York, 1943, ISBN 9780470172766.

[4] Eidevåg T., Thomson E.S., Kallin D., Casselgren J. and Rasmuson A. Angle of repose of snow: An experimental study on cohesive properties. *Cold Regions Science and Technology* (2022) **194**.

[5] Vallero, G., Barbero, M., Barpi, F., Borri-Brunetto, M., De Biagi, V., Ito, Y. and Yamaguchi, S. Experimental study of the shear strength of a snow-mortar interface *Cold Regions Science and Technology* (2022) **193**

[6] Sovilla, B., Sonatore, I., Bühler, Y. and Margreth, S. Wet-snow avalanche interaction with a deflecting dam: field observations and numerical simulations in a case study *Natural Hazards and Earth System Sciences* (2012) **12**:1407–1423.

[7] O'Rourke, M. *Snow loads : guide to the snow load provisions of ASCE 7-10*. ASCE Press, 2010, ISBN 9780784476109.

[8] Lang, R. *Algorithms for design and analysis of membrane structures*. Brno, 2019. Doctoral Thesis. Brno University of Technology. Supervisor Ivan Němec.

[9] GERLIC, K. Design Elements for Snow-Load Resistant Membrane Roofs. *Beyond the limits of man*, 1—6 (2013), ISSN 2518-6582.